SCIENTIFIC REPORTS

OPEN

How is water-use efficiency of terrestrial ecosystems distributed and changing on Earth?

Xuguang Tang[1], Hengpeng Li[1], Ankur R. Desai[2], Zoltan Nagy[3], Juhua Luo[1], Thomas E. Kolb[4], Albert Olioso[5], Xibao Xu[1], Li Yao[6], Werner Kutsch[7,8], Kim Pilegaard[9], Barbara Köstner[10] & Christof Ammann[11]

[1]State Key Laboratory of Lake Science and Environment, Nanjing Institute of Geography and Limnology, Chinese Academy of Sciences, Nanjing 210008, China, [2]Department of Atmospheric and Oceanic Sciences, University of Wisconsin-Madison, WI, USA, [3]MTA-SZIE Plant Ecology Research Group, Szent Istvan University, Pater K. 1., 2100 Gödöllő, Hungary, [4]School of Forestry, Northern Arizona University, Flagstaff, AZ 86011, USA, [5]UMR 1114, EMMAH (Environnement Méditerranéen et Modélisation des AgroHydrosystème), INRA-UAPV, F-84 914 Avignon Cedex 9, France, [6]School of Geographical Science, Northeast Normal University, Changchun 130024, China, [7]Institute for Climate-Smart Agriculture, Thünen-Institute, Bundesallee 50, 38116, Braunschweig, Germany, [8]ICOS Headoffice, Department of Physics, FI-00014 University of Helsinki, Finland, [9]Department of Chemical and Biochemical Engineering, Technical University of Denmark, Roskilde, Denmark, [10]Technische Universitat Dresden, Institute of Hydrology and Meteorology, Dresden, Germany, [11]Research Station Agroscope, Climate and Air Pollution Group, 8046 Zurich, Switzerland.

A better understanding of ecosystem water-use efficiency (WUE) will help us improve ecosystem management for mitigation as well as adaption to global hydrological change. Here, long-term flux tower observations of productivity and evapotranspiration allow us to detect a consistent latitudinal trend in WUE, rising from the subtropics to the northern high-latitudes. The trend peaks at approximately 51°N, and then declines toward higher latitudes. These ground-based observations are consistent with global-scale estimates of WUE. Global analysis of WUE reveals existence of strong regional variations that correspond to global climate patterns. The latitudinal trends of global WUE for Earth's major plant functional types reveal two peaks in the Northern Hemisphere not detected by ground-based measurements. One peak is located at 20° ～ 30°N and the other extends a little farther north than 51°N. Finally, long-term spatiotemporal trend analysis using satellite-based remote sensing data reveals that land-cover and land-use change in recent years has led to a decline in global WUE. Our study provides a new framework for global research on the interactions between carbon and water cycles as well as responses to natural and human impacts.

Plants in terrestrial ecosystems on Earth assimilate atmospheric CO_2 through photosynthesis, which is inherently accompanied with the loss of water through stomata that regulate the mass-energy exchange between the leaf and the atmosphere[1–2]. The rate of carbon uptake per unit of water lost, also called water-use efficiency (WUE), is an important parameter for understanding the metabolism of terrestrial ecosystems. Carbon and water fluxes of leaves are related to those of larger scale ecosystems, but fluxes at ecosystem scales are weakly constrained[3]. The question of how much water a plant uses relative to carbon gained has been examined in fields ranging from plant physiology to applied scientific disciplines such as irrigation science and agronomy[4]. Given ongoing climatic change and ecosystem degradation, a deeper understanding of whole ecosystem WUE will improve our ability to simulate and predict carbon and water cycles and to refine water management[5–6].

Owing to measurement difficulties, few studies have systematically compared global patterns of WUE of terrestrial ecosystems across different vegetation types or have analyzed the seasonal variability of WUE in relation to meteorological conditions. Ecosystem WUE is slightly different from plant WUE. Plant physiologists usually consider WUE at leaf or stand scales and are mainly interested in relations between total or above-ground biomass, stem biomass or net CO_2 uptake to transpiration or evapotranspiration (ET)[7–8]. Here, we use a whole ecosystem estimate of water use, evapotranspiration (ET), defined as the total water vapour flux between the canopy and the atmosphere consisting of evaporation from soil, plant transpiration and evaporation of the intercepted fraction. Major ecozones are often characterized with differing water-use efficiencies owing to inherent physiological variation in leaf gas exchange and environmental conditions. Our definition is similar to what ecologists commonly use for whole ecosystem WUE, which is the ratio of net primary production, net

1

ecosystem production, or gross ecosystem production to water use or evapotranspiration[4,9–10]. While the exchange of both CO_2 and water vapor is regulated by stomatal aperture for leaf-level WUE, ecosystem-level WUE is also affected by evaporation and vegetation morphology. This discrepancy complicates comparisons of WUE from different sources. Here we use the ecosystem-level definition, which is relevant for evaluating ecosystem models.

Further, variability in WUE can be evaluated at different time scales, ranging from diurnal, seasonal, to interannual[11]. The time scale of investigation needs to be determined primarily in order to quantify the different patterns of WUE and the underlying mechanisms in relation to vegetation types and meteorological conditions. Here, we analyzed the dynamics of WUE at both annual and seasonal time scales.

Also, WUE is dependent on the spatial unit of analysis. Water and carbon cycles usually occur heterogeneously over the land surface, which requires an appropriate upscaling methodology at regional and global scales. Although several studies have explored the interaction between water and carbon cycles[12–13], few global-scale analyses have been performed till now. Better quantification of global patterns of terrestrial WUE is needed to further understanding of natural and human impacts.

The seasonal dynamics of WUE differ strongly depending on location, climatic factors, plant functional type, species composition and disturbance history, requiring consistent, temporally continuous, and spatially distributed observations for accurate assessment of WUE. In addition to leaf-level measurements and inventory surveys[14–15], in recent years, with the development of the long-term eddy covariance technique, tower-based monitoring of ecosystem carbon and water cycles has made global evaluation of productivity, respiration, and evapotranspiration possible[16–18]. Data from hundreds of sites are cooperatively shared through the global network–FLUXNET[19–21]. Currently the FLUXNET community throughout the world has been running for more than two decades enabled scientists to assess terrestrial WUE and the determining environmental conditions at different time scales across numerous sites of diverse vegetation types precisely[3–4,22]. Although uncertainties associated with site-to-site variation in site quality criteria, flux measurement methods, calculations and data quality control still exist, ongoing standardization and quality assurance efforts enable global integration.

Satellite-based remote sensing of vegetation can be used to derive global WUE. NASA TERRA and AQUA MODIS-based estimates of gross primary production (GPP) and terrestrial evapotranspiration (ET) can be obtained to quantify large-scale WUE[23–24]. Tower-based measured WUE can be used to evaluate the reliability and accuracy of estimates of global WUE from satellite-based approaches.

The primary objectives of this study are 1) to investigate the latitudinal trend in WUE of terrestrial ecosystems across different plant functional types with data from FLUXNET; 2) to evaluate global patterns of terrestrial WUE using satellite remote sensing-based GPP and ET products, which provides a new framework for global research on carbon and water cycles.

In this study, we used measurements of CO_2 and H_2O fluxes combined with other hydrometric measurements of 32 sites covering six major plant functional types that represent the major ecozones of the northern Hemisphere. These sites range from 20°N to 70°N in latitude and provide 137 site-years in total (Table 1 and Fig. 1).

Despite the wide range of plant functional types and associated stand structures, soil types, stand age, site disturbance history and

Table 1 | FLUXNET sites used in this study

Sites	Longitude	Latitude	Plant functional type	LAI	Age	Year used
1 CN-DHS	112.57 E	23.17 N	Broad-leaved evergreen	4.25	old-growth	2003 ~ 2008
2 US-KS2	80.671 W	28.608 N	Broad-leaved evergreen	2.1	16	2004 ~ 2006
3 US-SP1	82.219 W	29.738 N	Needleleaf evergreen	3.4	80	2003 ~ 2006
4 US-Fmf	111.727 W	35.143 N	Needleleaf evergreen	1.2	~100	2005 ~ 2007
5 PT-Mi2	8.024 W	38.475 N	Grassland	~	~	2004 ~ 2008
6 ES-ES2	0.315 W	39.276 N	Crop	~	~	2004 ~ 2008
7 US-MMS	86.413 W	39.323 N	Broad-leaved deciduous	4.1	70	2003 ~ 2006
8 ES-ES1	0.319 W	39.346 N	Needleleaf evergreen	2.6	~100	2003 ~ 2006
9 IT-Cpz	12.377 E	41.705 N	Broad-leaved evergreen	3.5	38	2003 ~ 2008
10 IT-Col	13.588 E	41.849 N	Broad-leaved deciduous	5.5	114	2003 ~ 2010
11 ES-VDA	1.448 E	42.152 N	Grassland	~	~	2004 ~ 2008
12 CN-CBS	128.09 E	42.4 N	Mixed forest	3.5	~200	2003 ~ 2008
13 US-Ha1	72.172 W	42.538 N	Broad-leaved deciduous	4.7	75 ~ 110	2003 ~ 2006
14 FR-Avi	4.878 E	43.917 N	Crop	~	~	2004 ~ 2006
15 FR-LBr	0.769 W	44.717 N	Needleleaf evergreen	2.8	44	2003 ~ 2008
16 IT-Cas	8.668 E	45.063 N	Crop	~	~	2006 ~ 2010
17 US-Ho1	68.740 W	45.204 N	Needleleaf evergreen	5.6	109	2002 ~ 2004
18 US-Syv	89.347 W	46.242 N	Mixed forest	4.1	0 ~ 350	2002 ~ 2006
19 CH-Oe1	7.732 E	47.286 N	Grassland	~	~	2003 ~ 2008
20 CH-Oe2	7.734 E	47.286 N	Crop	~	~	2004 ~ 2006
21 FR-Hes	7.066 E	48.674 N	Broad-leaved deciduous	5.7	35	2003 ~ 2010
22 DE-Tha	13.567 E	50.964 N	Needleleaf evergreen	4.8	120	2003 ~ 2010
23 DE-Hai	10.452 E	51.079 N	Broad-leaved deciduous	4.8	0 ~ 250	2003 ~ 2007
24 DE-Geb	10.914 E	51.100 N	Crop	~	~	2003 ~ 2010
25 BE-Bra	4.521 E	51.309 N	Mixed forest	~	79	2007 ~ 2010
26 NL-Cal	4.927 E	51.971 N	Grassland	~	~	2003 ~ 2008
27 DK-Sor	11.644 E	55.486 N	Broad-leaved deciduous	4.7	84	2003 ~ 2008
28 DK-Ris	12.097 E	55.530 N	Crop	~	~	2004 ~ 2008
29 DK-Lva	12.083 E	55.683 N	Grassland	~	~	2004 ~ 2008
30 SE-Kno	16.217 E	60.998 N	Needleleaf evergreen	4.5	52	2006 ~ 2009
31 SE-Fla	19.456 E	64.113 N	Needleleaf evergreen	2.4	100	2001 ~ 2002
32 FI-Sod	26.637 E	67.362 N	Needleleaf evergreen	3.5	58 ~ 88	2007 ~ 2008

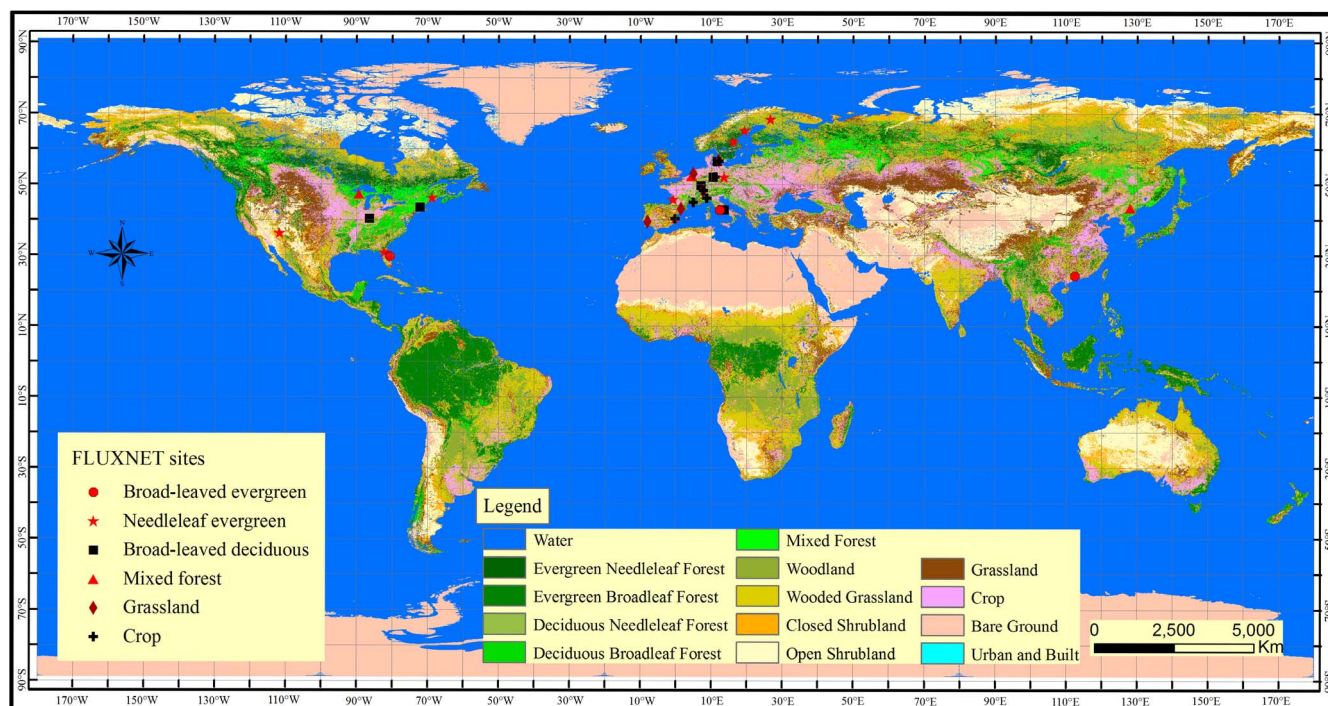The names of flux sites are abbreviations from the FLUXNET community.

Figure 1 | Locations of the 32 flux tower sites (see also Table 1) providing water-use efficiency data also used for validation of the remotely-sensed WUE product. The global land cover classification data is produced by Hansen et al. (2000) and can be downloaded from http://www.landcover.org/data/landcover/index.shtml This figure was produced using ArcGIS 10.1.

year-to-year variability, there is a clear and distinct latitudinal trend in WUE of terrestrial ecosystems (Fig. 2 and Table 2). The trends indicated that as the latitude rose from the subtropics to the northern high-latitudes, multi-year average WUE of all sites increased and reached a peak at approximately 51°N, and then tended to decline at higher latitudes. Although the peak magnitude of WUE differed among plant functional types, all peaks occur at approximately the same latitude, suggesting a key zonal differentiation rule driven by radiation and water availability. However, the tendency was also affected by the non-random coverage of terrestrial ecosystems, highlighting biological adaptations of WUE to specific climatic conditions. Indeed latitude is not a phenomenological driving variable per se, but is a proxy for the complicated effects of a multiplicity of abiotic and biotic factors, which determine the major ecozones.

While having similar latitudinal pattern, the magnitude of ecosystem WUE differed among plant functional groups (Fig. 3). Evergreen forests generally had higher WUE than deciduous vegetation types at similar latitudes. WUE of broad-leaved evergreen forest was higher than that of needleleaf evergreen forest. Both mixed forest and grassland had lower WUE than broad-leaved deciduous forest. However, the peak WUE value of grassland at 51°N was equivalent in magnitude to mixed forests. Crop sites had the lowest WUE among the terrestrial ecosystems, which indicated the high water utilization of food production systems relative to carbon gained, and has implications for agronomic crop breeding in dry-land farming and management of irrigation water. The lower annual WUE of crops could also be affected by non-productive phases with higher soil evaporation compared to permanent vegetation.
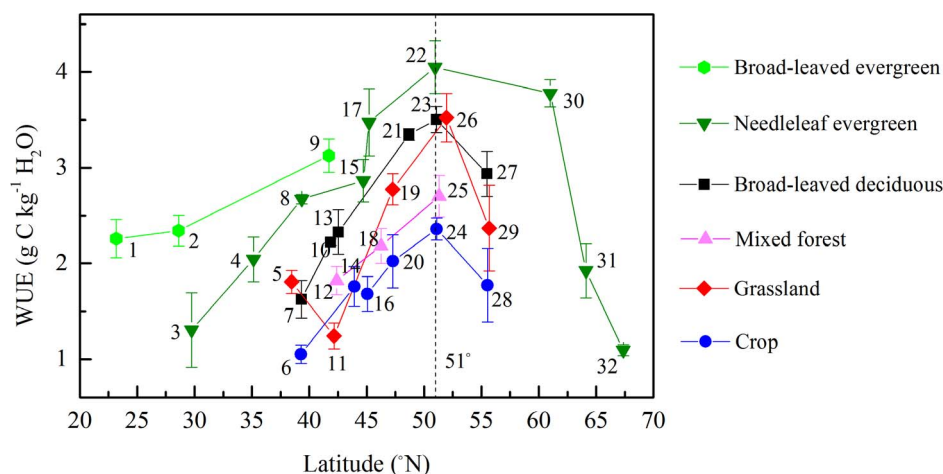

Figure 2 | Latitudinal trends in multiyear mean annual water use efficiency at the 32 sites for different plant functional types. The eddy covariance sites used were listed briefly in Table 1. The interannual variability is represented by the standard error bar. This figure was produced using Origin 8.0.

Table 2 | Multiyear mean annual water use efficiency (WUE) and the standard deviation (SD) at the 32 sites for different plant functional types (PFT)

PFT	Site	Mean WUE (g C kg^{-1} H$_2$O)	SD (g C kg^{-1} H$_2$O)	PFT	Site	Mean WUE (g C kg^{-1} H$_2$O)	SD (g C kg^{-1} H$_2$O)
Broad-leaved evergreen forest	CN-DHS	2.26	0.201	Broad-leaved deciduous forest	US-MMS	1.625	0.196
	US-KS2	2.345	0.161		IT-Col	2.222	0.034
	IT-Cpz	3.126	0.175		US-Ha1	2.329	0.232
Needleleaf Evergreen forest	US-SP1	1.304	0.390		FR-Hes	3.348	0.062
	US-Fmf	2.044	0.235		DE-Hai	3.504	0.136
	ES-ES1	2.672	0.048		DK-Sor	2.937	0.236
	FR-LBr	2.865	0.222	Mixed forest	CN-CBS	1.820	0.146
	US-Ho1	3.474	0.351		US-Syv	2.183	0.183
	DE-Tha	4.050	0.276		BE-Bra	2.704	0.217
	SE-Kno	3.777	0.143	Crop	ES-ES2	1.051	0.097
	SE-Fla	1.924	0.284		FR-Avi	1.759	0.209
	FI-Sod	1.095	0.057		IT-Cas	1.681	0.180
Grassland	PT-Mi2	1.807	0.120		CH-Oe2	2.023	0.278
	ES-VDA	1.242	0.136		DE-Geb	2.361	0.115
	CH-Oe1	2.775	0.163		DK-Ris	1.773	0.383
	NL-Cal	3.523	0.253				
	DK-Lva	2.369	0.450				

The names of flux sites are abbreviations from the FLUXNET community.

To further investigate the global patterns of terrestrial water-use efficiency, we also used satellite remote sensing-based data from the recently revised MODIS GPP and newly developed ET products between 2000 and 2013. These were used to infer mean annual terrestrial WUE over a period that closely corresponds to tower-based measured WUE. Multiyear mean annual GPP, ET, and WUE showed strong regional variations corresponding to climatic variations in water availability but still presented consistent latitudinal gradients similar to data from the tower network (Fig. 4). Spatially, terrestrial WUE increases from low latitudes to high latitudes in the North America and Eurasia continents, and tends to decline after reaching the peak values in the boreal regions, though slightly further north than the towers showed.

Ecosystems dominated by evergreen PFT at low latitudes adjacent to Pacific West Coast and Atlantic West Coast have high WUE. Alpine plateaus in Northwest China, African deserts, and the Cordillera that runs along the western edge of North and South America showed markedly low WUE. The trough of WUE for needleleaf evergreen forest was found in the southeastern region of the United States and China's central and western regions, and the peak was found in Northern Eurasia and northwestern North America. For broad-leaved deciduous forest, the minimum WUE is located at China's central and western regions whereas the maximum WUE is located in Northwest Russia. Grassland is mainly distributed between 45° ～ 55°N, and the peak of WUE is situated at Southeast Alaska, North Europe and Southeast Russia. Cropland maximum WUE appears in Central Europe, southern Canada and South Russian.

We also compared the global MODIS-based calculation of GPP, ET and WUE with other proxies[25–27]. Compared with the global estimates of GPP (123 ± 8 Gt C/year) by Beer et al. (2010)[25] using eddy covariance flux data and various diagnostic models, the present
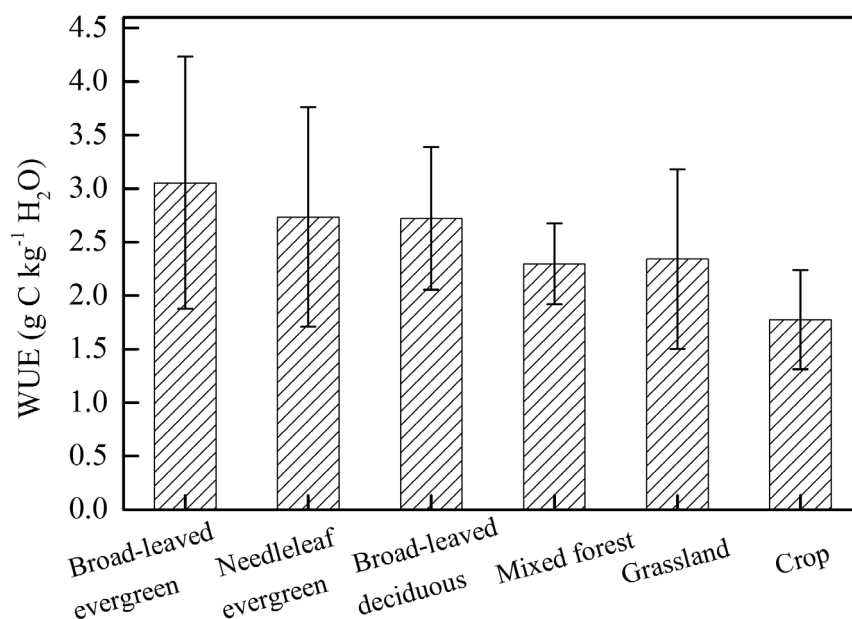

Figure 3 | Comparison of multiyear mean annual water use efficiency among the main plant functional types. Interannual variation of per plant functional type is represented by the standard error bar. This figure was produced using Origin 8.0.
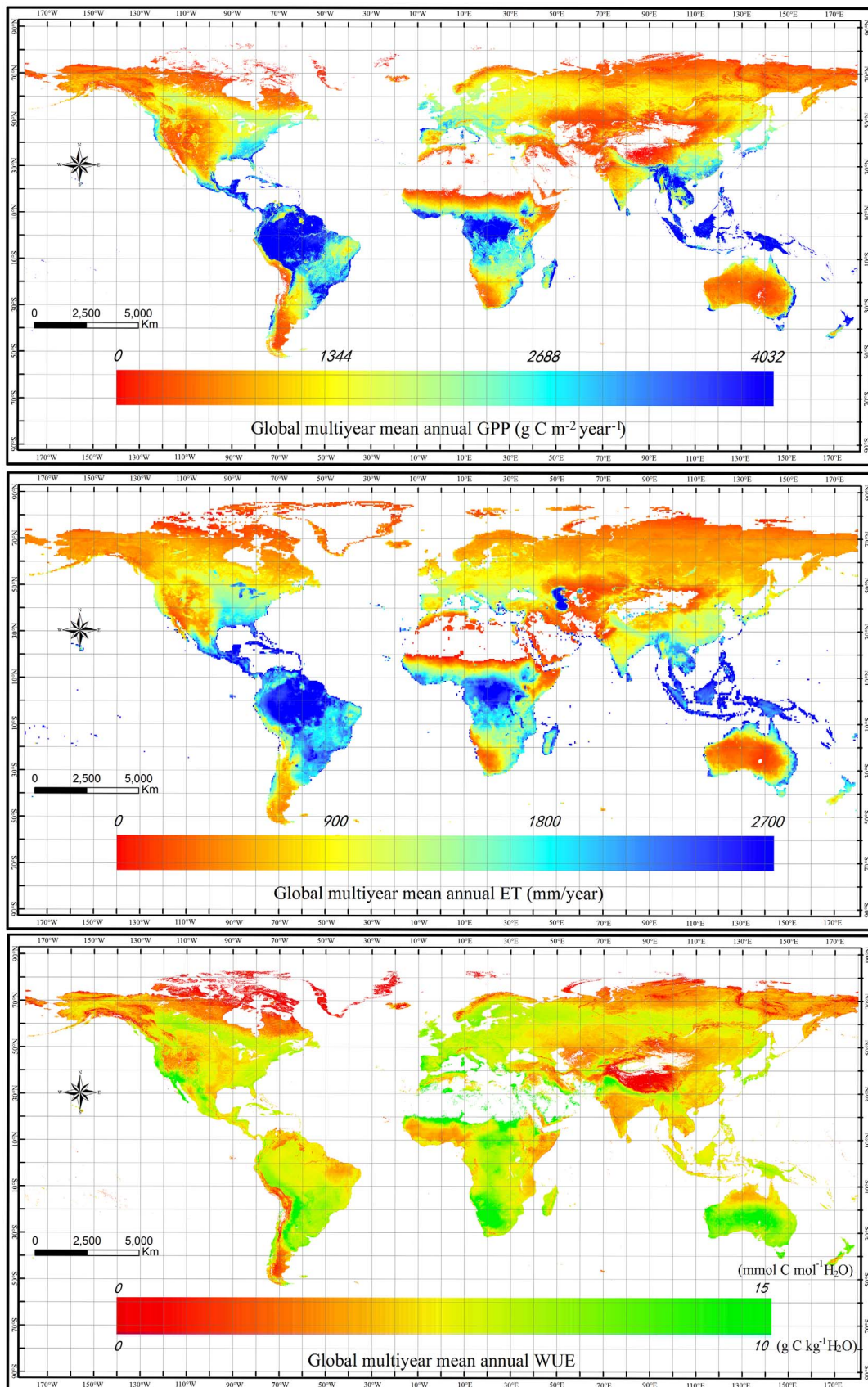
Figure 4 | Global distribution of multiyear mean annual GPP, ET and WUE in the study period. Bare ground and ocean areas were excluded from the model calculations. This figure was produced using ArcGIS 10.1.
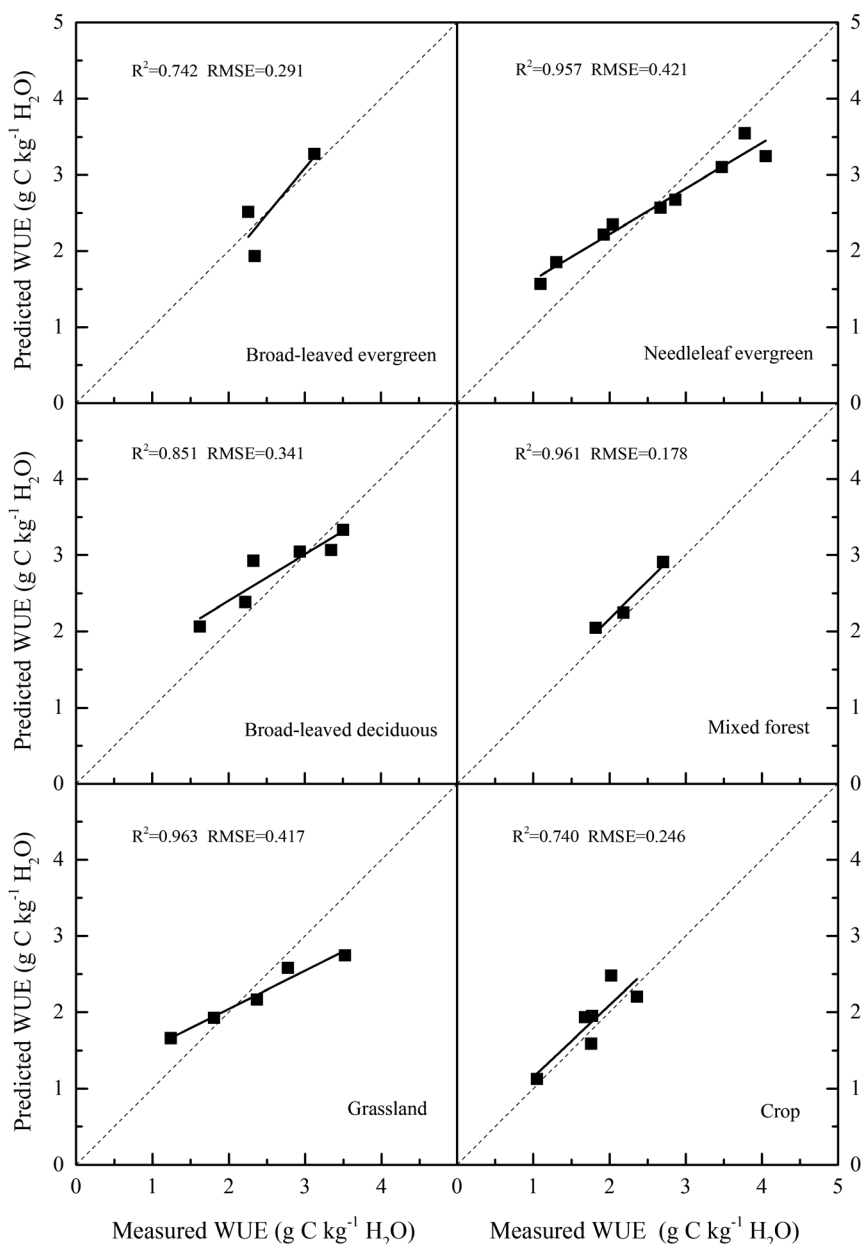
Figure 5 | Comparisons between tower-based measured WUE and remotely-sensed modeled WUE product at the 32 sites for the plant functional types. This figure was produced using Origin 8.0.

study showed multiyear mean annual GPP (during 2000 ~ 2013) of 156.82 Gt C/year. Jung et al. (2011)[26] estimated a mean annual global land-surface ET value from 1982 to 2008 of $65 \pm 3 \times 10^3$ km³/year and Miralles et al. (2011)[28] found that annual land evaporation was estimated as 67.9×10^3 km³ during the period 2003 to 2007, 80% corresponding to transpiration, 11% to interception loss, 7% to bare soil evaporation and 2% snow sublimation, whereas multiyear mean annual ET from MODIS during 2000 to 2013 was $90.8 \pm 1.2 \times 10^3$ km³/year. It could be partly explained by the coarse resolution of previous studies (1/2 degree in Jung et al. 2011 and 1/4 degree by Miralles et al. 2011) which might lead to small-scale features being neglected. Although our global GPP and ET estimates are significantly larger than previous studies, WUE from MODIS and by combining the GPP and ET estimates above were quite similar, globally at 1.89 g C kg⁻¹ H₂O (2.83 mmol C mol⁻¹ H₂O) from the tower upscaling and 1.71 g C kg⁻¹ H₂O (2.56 mmol C mol⁻¹ H₂O) by MODIS remote sensing. Therefore, our results showed the consistent estimates between tower- and remote-sensing approaches of global WUE.

To evaluate the reliability and accuracy of the satellite-based global WUE product, tower-based measured WUE data at these 32 sites were used for validation. Although the number of flux sites was limited for each vegetation type and occasionally large differences occurred between remotely-sensed WUE and measured WUE for individual points, the satellite-based WUE product was relatively accurate on a global basis (Fig. 5). A well-calibrated model should have a root mean square error (RMSE) that is small relative to the total observed variation and an R^2 close to 1. Remotely-sensed WUE of mixed forest compared closely with the tower-measured WUE (RMSE = 0.178 g C kg⁻¹ H₂O; R^2 = 0.961), while the overall bias of grassland and evergreen needleleaf forest was worse. Accuracies for crop, evergreen broadleaf forest and deciduous broadleaf forest were intermediate between these two extremes.

We also compared our estimates of ecosystem WUE with estimates of plant WUE. Jasechko et al. (2013)[29] used literature estimates of WUE and a watershed isotope estimate of transpiration and developed a global map of plant water use efficiency (GPP/transpira-
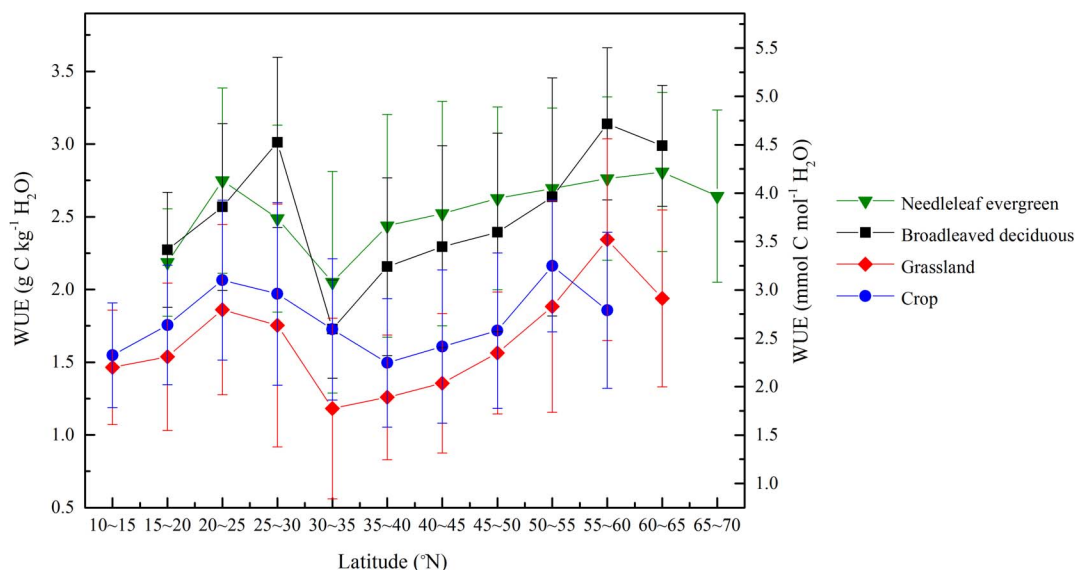
Figure 6 | Latitudinal evolution of global WUE for the main plant functional types in the Northern Hemisphere. Every 5 degrees in latitude was divided into an independent evaluation unit. The spatial variability in each unit is represented by the standard error bar. This figure was produced using Origin 8.0.

tion). This map shows that evapotranspiration exceeds transpiration by 2/3 in most terrestrial ecosystems, and patterns of global WUE were similar to our estimates of ecosystem WUE based on satellite data. This comparison shows that our estimates of ecosystem WUE can serve as a proxy for plant WUE. Ecosystem WUE also provides a more general measurement of total water use by an ecosystem, as to some extent plant canopy cover influences land surface evaporation, and adaptive processes may lead to plant canopy characteristics that minimize evaporation by limiting soil radiation exposure, for example.

There are some differences between the satellite estimate of the WUE-latitude trend and the tower observations (Fig. 6). Unlike the flux tower latitudinal gradient, however, remote sensing analysis revealed two peaks in WUE trends for four vegetation types. For needleleaf evergreen forest, grassland and crop, the first peak occurred at $20° \sim 25°$N while this peak was a little farther north ($25° \sim 30°$N) for broad-leaved deciduous forest. Apart from that, the tendency of ecosystem-level WUE was similar to latitudinal zonality found using flux measurements. The northern peaks of WUE in the satellite observations were located at $60° \sim 65°$N for needleleaf evergreen forest, $55° \sim 60°$N for broad-leaved deciduous forest and grassland, and $50° \sim 55°$N for cropland, respectively. The distinct differences in spatial patterns of WUE among various ecosystems imply an additional biological constraint over latitudinal radiation availability conditions.

The seasonal pattern of WUE by site reveals how mechanisms that lead to long-term annual WUE vary by plant functional type (Fig. 7). WUE was higher at the beginning and end of the year, and lowest in summer in broad-leaved evergreen forest except for an Italian Mediterranean site (IT-Cpz) where the relatively low temperature during winter months hindered the growth of vegetation. Similarly, needleleaf evergreen forest showed significant peaks during early growing season (spring) and late growing season (late summer). In contrast, a consistent tendency was found in both mixed forest and broad-leaf deciduous forest of a singe WUE peak in summertime. The seasonal dynamics in WUE of grassland lacked consistent patterns owing to the broadly-distributed location of grasslands among various climate patterns and both C_3 and C_4 photosynthetic pathways. Crop WUE is likely also sensitive to the variety of farming systems.

The northern peak value of WUE appears to be driven by the effect of evaporation and transpiration, which both decrease with latitude (driven by net radiation) while vegetation productivity peaks for boreal forests in mid- and high latitudes (driven by solar radiation in summer). Boreal systems are in the 'sweet spot' of cool conditions that limit water loss and high incoming radiation in summer to maximize photosynthetic uptake. To identify the main factors controlling WUE for each plant functional type and the underlying mechanism, the relationships between terrestrial WUE with the corresponding global radiation (R_g), air temperature (T_a), vapour pressure deficit (VPD), soil temperature (T_s), precipitation (P_r) and soil water content (SWC) were compared (Table 3). Radiation and temperature were negatively correlated with WUE for broad-leaved evergreen forest, whereas soil water content was positively correlated. However, for other ecosystems, the meteorological conditions including radiation, temperature, and vapor pressure deficit have a strong positive correlation with water-use efficiency, which partly explains differences among tropics (operating at near optimum temperature and radiation conditions) and temperate systems (temperature and light limited). For broad-leaved deciduous forest and grassland, SWC showed significantly negative correlation with WUE, whereas it was weakly negative for crop and needleleaf evergreen forest. Temperature and vapor pressure deficit are the most important meteorological factors that drive WUE.

Given increases in urbanization land accompanying by reduction in vegetation cover over the world, we would predict that continued land-cover and land-use change on Earth leads to a decline in global WUE. However, the temporal trend in WUE is affected by a suite of co-varying natural factors and human activities. Keenan et al. (2013)[3] found a substantial increase in WUE in temperate and boreal forests of the Northern Hemisphere as atmospheric carbon dioxide concentrations rose over the past two decades. However, these analyses were based on site-level measurements. Our analysis of the 2000–2013 MODIS time-series of global annual mean WUE indicated a distinctly decreasing tendency that might be correlated with land-use changes (Fig. 8). But the declining trend of WUE has changed direction in the past 4 years, perhaps reflecting CO_2 fertilization and climate warming effects or just interannual variability. Donohue et al. (2013)[30] also found the significant impact of CO_2 fertilization on maximum foliage cover across the globe's warm, arid environments
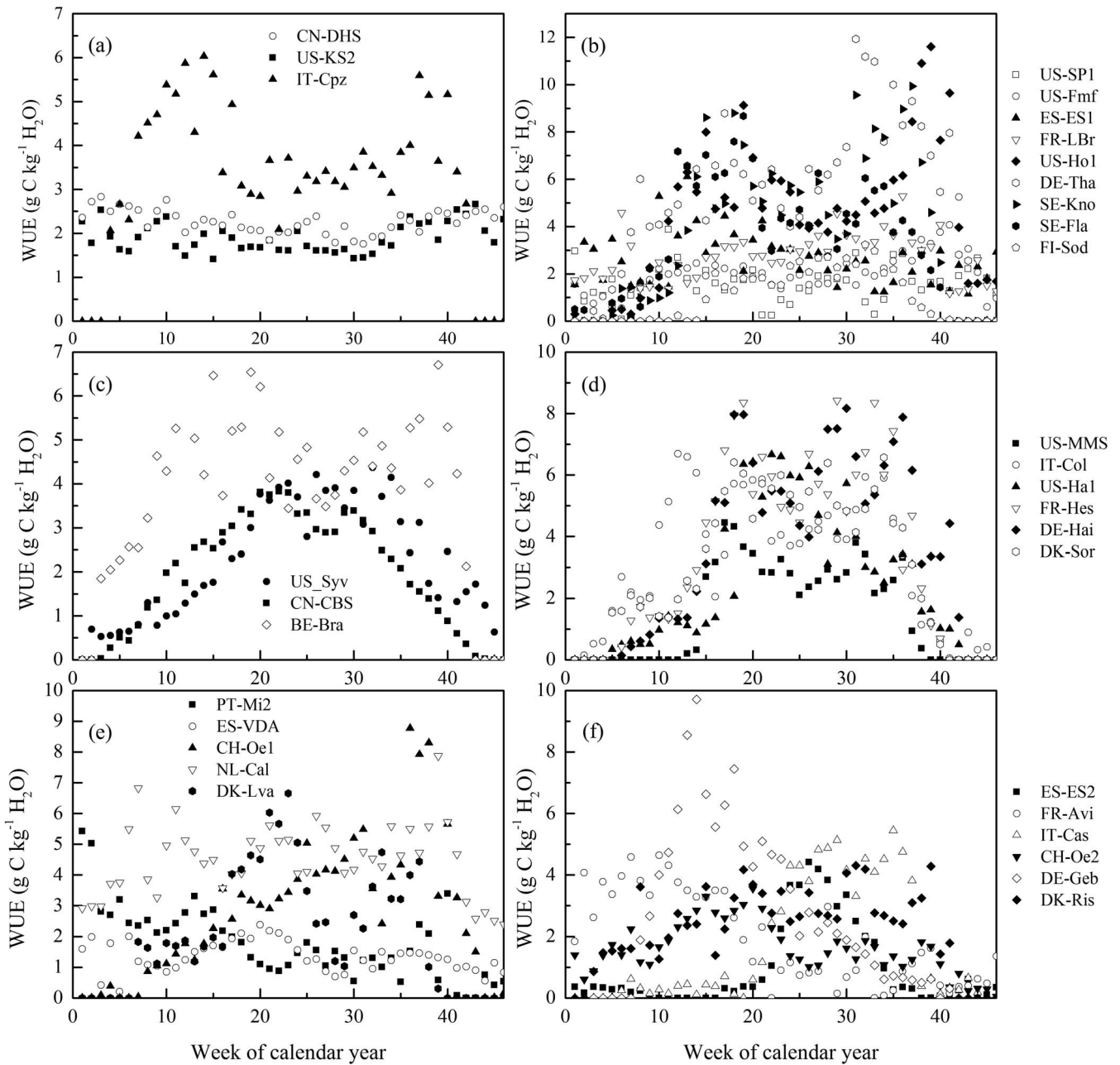
Figure 7 | Seasonal dynamics of terrestrial water use efficiency of the FLUXNET sites used in Table 1 according to the plant functional types at 8-day time scale. These EC sites were listed briefly in Table 1. (a) broad-leaved evergreen forest; (b) needleleaf evergreen forest; (c) mixed forest; (d) broad-leaved deciduous forest; (e) grassland and (f) cropland. This figure was produced using Origin 8.0.

Table 3 | Correlation analysis between water use efficiency and the controlling environmental factors in terrestrial ecosystems according to plant functional types

	Plant functional type	R_g	T_a	VPD	T_s	P_r	SWC
WUE	Broad-leaved evergreen	−0.645**	−0.600**	−0.669**	−0.606**	0.151	0.541**
	Needleleaf evergreen	0.599**	0.795**	0.524**	0.808**	−0.092	−0.178
	Broad-leaved deciduous	0.631**	0.739**	0.483**	0.786**	0.234	−0.633**
	Mixed forest	0.730**	0.901**	0.783**	0.925**	0.212	0.136
	Grassland	0.597**	0.594**	0.574**	0.670**	−0.096	−0.442**
	Crop	0.525**	0.693**	0.504**	0.688**	−0.172	−0.228

**Correlation is significant at the 0.01 level. R_g refers to global radiation. T_a refers to air temperature. VPD refers to vapour pressure deficit. T_s refers to soil temperature. P_r refers to precipitation. SWC refers to soil water content.
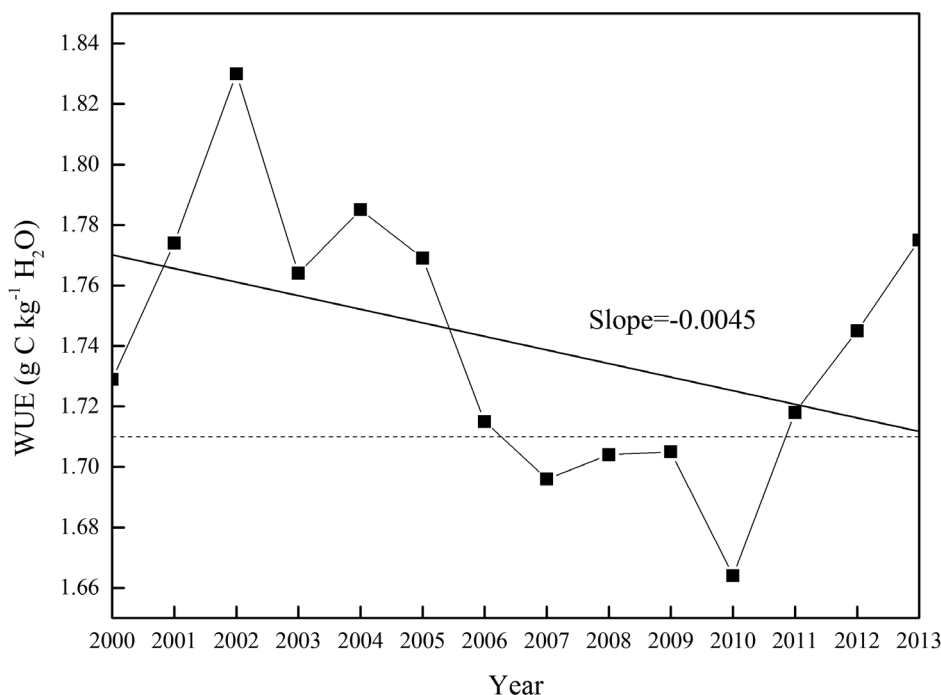
Figure 8 | Trend analysis of time-series global annual mean WUE for 2000–2013. The dashed line refers to multiyear mean annual value of WUE during this period.

and this effect was occurring alongside ongoing anthropogenic perturbations to the carbon cycles.

Silva & Anand (2013)[31] investigated the influence of atmospheric CO_2 concentration and climate warming on tree growth and intrinsic water use efficiency (iWUE) based on a synthesis of the literature of site-level measurements, and found that responses in growth are latitude dependent with temporal changes in iWUE. Moreover, they identified positive relationships between iWUE and tree growth in boreal and Mediterranean forests located in latitudes greater than 40°N, with progressively lower responses toward lower latitudes. In this respect, these research results are consistent with our global time-series trend analysis. In addition, Silva & Horwath (2013)[32] found that previously reported trend in iWUE cannot reflect a coherent global response to rising atmospheric CO_2 and our present study indicated a distinctly decreasing tendency in global WUE during the past decade in spite of rising CO_2 concentration owing to natural and human activities.

In addition, WUE trends in C_3 and C_4 plants differ. Plant water use efficiency has been shown to vary between photosynthetic pathways and C_4 vegetation showed increasing water use efficiency in response to rising levels of atmospheric CO_2 with consistent reductions in stomatal conductance and transpirational water loss compared to C_3 species. Still et al. (2003)[33] developed the C_3/C_4 distribution by combining remote sensing products, physiological modeling, a spatial distribution of global crop fractions, and national harvest area data for major crop types. Therefore, by comparing with global patterns of WUE, distribution of C_4 vegetation, and vegetation type map in Fig. 1, we can find that 1) the C_4 vegetation mainly occurs in the vast tropical and subtropical grassland and savanna regions. Temperate grassland regions in North and South America and Africa also contain high fractional C_4 coverage whereas it is only found in a very small fraction throughout temperate Eurasia and in the upper Great Plains region of North America; 2) although the C_4 vegetation have impact on predictions of GPP and WUE with changing climate, global trend analysis is affected by a suite of natural factors and human activities and the mix of vegetation, which is dominated by C_3 responses. Currently it appears that recent trends

of global WUE were more controlled by land use and land cover changes from human disturbances.

Flux observations in terrestrial ecosystems across different plant functional types reveals a consistent latitudinal zonality in WUE from the subtropics to the northern high-latitudes, peaking at approximately 51°N and then tending to decline at higher latitude. Though WUE from individual site shows large variation, the overall latitudinal trend observed in each vegetation type proved to be a persistent one. The latitudinal gradient in WUE was consistent among various estimates of WUE, whether by satellite or tower, though subtle difference in location of the peak WUE and regions of very high or low WUE differed. Satellite remote sensing provides a new tool for the global research on role of WUE and monitoring how WUE responds to changing environmental conditions. Decreasing WUE globally in the last decade may reflect land use change as well as other poorly understood factors. Our understanding of the large-scale processes determining terrestrial WUE is still insufficient. The water and carbon cycles usually occur heterogeneously over the land surface, which requires an appropriate upscaling methodology at the regional and even global scales. Although several model studies have explored the interaction between water and carbon cycles, few global-scale analyses have been performed. Our analysis of global patterns of terrestrial WUE will be helpful to analyze ecosystem responses to natural and human impacts.

Methods

To estimate and analyze the global patterns of terrestrial water-use efficiency, we also used the remotely-sensed data from MODIS gross primary production (GPP) and developed ET at the global scale. The old Collection 4 GPP product was found to have considerable errors due to problems in the inputs. Zhao et al (2005)[23] rectified these products by improving the data processing methods and modifying parameters in the algorithm used, which generated the improved Collection 5 (C5) MOD17 estimates. The 8-day composite 1-km fraction of photosynthetically active radiation (FPAR) and leaf area index (LAI) data from the MODIS sensor were used as remotely sensed vegetation property dynamic inputs to the algorithm. Data gaps in the 8-day temporal MODIS FPAR/LAI caused by cloudiness were filled with information from accompanying quality-assessment flags. For daily meteorological data required to drive the algorithm, 6-hourly National Center for Environmental Prediction/ Department of Energy (NCEP/DOE) reanalysis II data were implemented. Monthly and annual GPP averages were derived by summing up each 8-day period. In addition, Mu et al. (2011)[24] improved a satellite remote sensing-based ET algorithm to assess global terrestrial ET using MODIS and global meteorology data by 1) simplifying the calculation of vegetation cover fraction; 2) calculating ET as the sum of daytime and nighttime components; 3) adding soil heat flux calculation; 4) improving estimates of stomatal conductance, aerodynamic resistance and boundary layer resistance; 5) separating dry canopy surface from the wet; and 6) dividing soil surface into saturated wet surface and moist surface. These data can be obtained freely from http://www.ntsg.umt.edu/project/mod16. Global land cover classification product at 1 km resolution developed by the University of Maryland was used to assist in extracting the latitudinal evolution of WUE for each biome (http://glcfapp.glcf.umd.edu:8080/esdi/index.jsp)[39].

Data treatment and statistical analysis. Water-use efficiency is calculated in various ways according to different scientific disciplines[4,6]. To systematically analyze the global patterns of terrestrial WUE on Earth and explore the key zonal differentiation rule along latitude across different plant functional types, we defined the WUE at the ecosystem scale as: $WUE = GPP/ET$. The seasonal trend of WUE was characterized by the weekly WUE (g C kg^{-1} H$_2$O). The measured latent heat (LE, w/m^2) fluxes were used to obtain water loss (ET, mm/day) by multiplying a factor of 0.035 which was converted by the formula $ET = LE/\lambda$ (λ represents amount of energy to evaporate a unit weight of water; 2454000 J kg^{-1}). The mean annual WUE value of each flux tower site was calculated as a proxy. The interannual variability is represented by the standard error. R^2 and RMSE were used to test the goodness of the satellite product at tower sites.

1. Field, C. B., Jackson, R. B. & Mooney, H. A. Stomatal responses to increased CO$_2$: implications from the plant to the global scale. *Plant Cell Environ.* **18**, 1214–1225 (1995).
2. Berry, J. A., Beerling, D. J. & Franks, P. J. Stomata: key players in the earth system, past and present. *Curr. Opin. Plant Biol.* **13**, 232–239 (2010).
3. Keenan, T. F. *et al.* Increase in forest water-use efficiency as atmospheric carbon dioxide concentrations rise. *Nature.* **499**, 324–327 (2013).
4. Kuglitsch, F. G. *et al.* Characterisation of ecosystem water-use efficiency of european forests from eddy covariance measurements. *Biogeosciences Discuss.* **5**, 4481–4519 (2008).
5. Chapin, F. S. III. *et al.* Ecosystem stewardship: sustainability strategies for a rapidly changing planet. *Trends Ecol. Evol.* **25**, 241–249 (2010).
6. Ito, A. & Motoko, I. Water-use efficiency of the terrestrial biosphere: a model analysis focusing on interactions between the global carbon and water cycles. *J. Hydrometeor.* **13**, 681–694 (2012).
7. Jarvis, P. G. Scaling processes and problems. *Plant Cell Environ.* **18**, 1079−1089 (1995).
8. Bacon, M. A. [Water use efficiency in plant biology] *What is water-use efficiency?* [Jones, H. G.] [27–41] (Blackwell Publishing, Oxford, 2004).
9. Law, B. E. *et al.* Environmental controls over carbon dioxide and water vapor exchange of terrestrial vegetation. *Agric. Forest Meteorol.* **113**, 97–120 (2002).
10. Luyssaert, S. *et al.* CO$_2$ balance of boreal, temperate, and tropical forests derived from a global database. *Glod. Change Biol.* **13**, 2509–2537 (2007).
11. Linderson, M. L., Iritz, Z. & Lindroth, A. The effect of water availability on stand-level productivity, transpiration, water use efficiency and radiation use efficiency of field-grown willow 20 clones. *Biomass Bioenerg.* **31**, 460–468 (2007).
12. Krinner, G. *et al.* A dynamic global vegetation model for studies of the coupled atmosphere-biosphere system. *Global Biogeochem. Cy.* **19**, GB1015 (2005).
13. Alton, P. *et al.* Simulations of global evapotranspiration using semiempirical and mechanistic schemes of plant hydrology. *Global Biogeochem. Cy.* **23**, GB4023 (2009).
14. Wullschleger, S. D., Tschaplinski, T. J. & Norby, R. J. Plant water relations at elevated CO$_2$ – implications for water-limited environments. *Plant Cell Environ.* **25**, 319–331 (2002).
15. Steduto, P., Hsiao, T. & Fereres, E. On the conservative behavior of biomass water productivity. *Irrig. Sci.* **25**, 189–207 (2007).
16. Valentini, R. *et al.* Respiration as the main determinant of carbon balance in European forests. *Nature* **404**, 861–865 (2000).
17. Peñuelas, J., Canadell, J. G. & Ogaya, R. Increased water-use efficiency during the 20th century did not translate into enhanced tree growth. *Global Ecol. Biogeogr.* **20**, 597–608 (2011).
18. Tang, X. G. *et al.* Estimating the net ecosystem exchange for the major forests in the northern United States by integrating MODIS and AmeriFlux data. *Agric. Forest Meteorol.* **156**, 75–84 (2012).
19. Running, S. A blueprint for improved global change monitoring of the terrestrial biosphere. *Earth Obs.* **10**, 8–12 (1998).
20. Yu, G. R., Wang, Q. F. & Zhu, X. J. Methods and uncertainties in evaluating the carbon budgets of regional terrestrial ecosystems. *Prog. Geog.* **30**, 103–113 (2011).
21. Barman, R., Jain, A. K. & Liang, M. Climate-driven uncertainties in modeling terrestrial gross primary production: a site level to global-scale analysis. *Glod. Change Biol.* **20**, 1394–1411 (2014).
22. Beer, C. *et al.* Temporal and among-site variability of inherent water use efficiency at the ecosystem level. *Global Biogeochem. Cy.* **23**, GB2018 (2009).
23. Zhao, M. *et al.* Improvements of the MODIS terrestrial gross and net primary production global data set. *Remote Sens. Environ.* **95**, 164–176 (2005).
24. Mu, Q. Z. *et al.* Improvements to a MODIS global terrestrial evapotranspiration algorithm. *Remote Sens. Environ.* **115**, 1781–1800 (2011).
25. Beer, C. *et al.* Terrestrial gross carbon dioxide uptake: global distribution and covariation with climate. *Science.* **5993**, 834–838 (2010).
26. Jung, M. *et al.* Recent decline in the global land evapotranspiration trend due to limited moisture supply. *Nature.* **7318**, 951–954 (2010).
27. Miralles, D. G. *et al.* El Niño-La Niña cycle and recent trends in continental evaporation. *Nature Climate Change.* **4**, 122–126 (2014).
28. Miralles, D. G. *et al.* Magnitude and variability of land evaporation and its components at the global scale. *Hydrol. Earth Syst. Sci.* **15**, 967–981 (2011).
29. Jasechko, S. *et al.* Terrestrial water fluxes dominated by transpiration. *Nature.* **7445**, 347–350 (2013).
30. Donohue, R. J. *et al.* Impact of CO$_2$ fertilization on maximum foliage cover across the globe's warm, arid environments. *Geophys. Res. Lett.* **40**, 3031–3035 (2013).
31. Silva, L. C. R. & Anand, M. Probing for the influence of atmospheric CO$_2$ and climate change on forest ecosystems across biomes. *Global Ecol. Biogeogr.* **22**, 83–92 (2013).
32. Silva, L. C. R. & Horwath, W. R. Explaining global increases in water use efficiency: why have we overestimated responses to rising atmospheric CO$_2$ in natural forest ecosystems? *PloS one.* **8**, e53089 (2013).
33. Still, C. J. *et al.* Global distribution of C$_3$ and C$_4$ vegetation: carbon cycle implications. *Global Biogeochem. Cy.* **17**, GB1817 (2003).
34. Reichstein, M. *et al.* Severe drought effects on ecosystem CO$_2$ and H$_2$O fluxes at three Mediterranean evergreen sites: revision of current hypotheses? *Glob. Change Biol.* **8**, 999–1017 (2002).
35. Zhu, X. J. *et al.* Seasonal dynamics of water use efficiency of typical forest and grassland ecosystems in China. *J. For. Res.* **19**, 70–76 (2014).
36. Lu, X. L. & Zhuang, Q. L. Evaluating evapotranspiration and water-use efficiency of terrestrial ecosystems in the conterminous United States using MODIS and AmeriFlux data. *Remote Sens. Environ.* **114**, 1924–1939 (2010).
37. Reichstein, M. *et al.* On the separation of net ecosystem exchange into assimilation and ecosystem respiration: review and improved algorithm. *Glob. Change Biol.* **11**, 1424–1439 (2005).
38. Moffat, A. M. *et al.* Comprehensive comparison of gap-filling techniques for eddy covariance net carbon fluxes. *Agric. Forest Meteorol.* **147**, 209–232 (2007).
39. Hansen, M. R. *et al.* Global land cover classification at 1km resolution using a decision tree classifier. *Int. J. Remote Sens.* **21**, 1331–1365 (2000).

Acknowledgments

Author contributions

T.X.G. and L.H.P. contributed equally to design this study and wrote this manuscript. A.R.D., Z.N., L.J.H., T.E.K., A.O., X.X.B., Y.L., K.P., B.K., C.A. and W.K. contributed significantly to the discussion of results and manuscript refinement. T.X.G. performed the analysis, and generated the figures and tables in the main text.

Additional information